Published by
NIGERIAN SOCIETY OF PHYSICAL SCIENCES
Available online @ https://journal.nsps.org.ng/index.php/jnsps

J. Nig. Soc. Phys. Sci. 5 (2023) 915

Journal of the Nigerian Society of Physical Sciences

Corrosion Inhibition Potential of Thiosemicarbazide Derivatives on ALuminium: Insight from Molecular Modelling and QSARs Approaches

B. T. Ogunyemi[a,*], F. K. Ojo[b]

[a]*Physical and Computational Chemistry Unit, Department of Chemistry, Federal University Otuoke, Bayelsa State, Nigeria*
[b]*Department of Chemistry, Bingham University, Karu Nasarawa State, Nigeria*

Abstract

The potentials of six thiosemicarbazide derivatives towards corrosion inhibition were investigated theoretically using density functional theory (DFT) and quantitative structural-activity relationships (QSARs) methods. Their performance as corrosion inhibitors were evaluated using their calculated quantum chemical parameters such as molecular weight, softness, electronegativity, dipole moments, hardness, bandgap energy (ΔE), highest occupied molecular orbital energy (E_{HOMO}), and the lowest unoccupied molecular orbital energy (E_{LUMO}). Regression analysis was carried out using the ordinary least square method to develop a model that establishes the relationship between chemical parameters and inhibition efficiencies that have been measured experimentally. According to the results, quantum chemical parameters confirm the inhibition potential of TSC_5 to be greater than TSC_2, while the predicted inhibition efficiencies of the studied thiosemicarbazide derivatives correspond to experimentally reported values with a root mean square error (%) of 1.116 and correlation coefficient of 0.998. The high correlation demonstrates and validates the quantum chemical approach's reliability in studying corrosion inhibition on a metal surface. The validation of the developed model internally and externally demonstrates that it is robust and stable, with high predictability.

DOI:10.46481/jnsps.2023.915

Keywords: DFT, Corrosion inhibitors, QSAR, Thiosemicarbazide

Article History :
Received: 04 July 2022
Received in revised form: 04 November 2022
Accepted for publication: 07 December 2022
Published: 14 January 2023

Communicated by: T. Owolabi

1. Introduction

Metals are utilized in most constructional operations because of their high strength contrasted with other material classes. However, the pace at which these metals revert to their natural oxide form, a process known as corrosion, has far-reaching implications for national economies and human life in general. Although, corrosion is unavoidable yet substantial barriers in form of corrosion control technology can be utilized to slow it down. Over the years, painting, cathodic and anodic protection, galvanizing, and the use of corrosion inhibitors (CIs), have been explored to alleviate the corrosion problem [1-2]. Corrosion inhibitors are commonly used in industry because of their low cost and ease of application [3-4]. Through molecule adsorption, the corrosion inhibitor forms a passive coating that protects the metal from aggressive corrosion thus limiting the rate of corrosion. Rather than utilizing high-grade carbon steel,

*Corresponding author tel. no: +234 8035811574
Email address: ogunyemibt@fuotuoke.edu.ng, btogunyemi@yahoo.com (B. T. Ogunyemi)

corrosion inhibitors have permitted lower-grade carbon steel to be utilized, thus lowering capital costs in most industries [3]. Aside from this, organic inhibitors are often employed due to their low toxicity, good solubility, compatibility with metals, and effectiveness at a wide temperature range [5-6].

The efficiency of organic corrosion inhibitors to inhibit corrosion largely depends on the adsorption bond strength which in turn depends on many factors such as type of metal, type of inhibitor, the concentration of inhibitor, and the environment. Besides these variables, most of the notable organic corrosion inhibitors are plane conjugated systems that include various aromatic cycles containing electronegative atoms [7]. Adsorption occurs as a result of the interaction of the inhibitor's lone pair and/or -orbitals with the metal surface atoms' d-orbitals, resulting in higher adsorption of the inhibitor molecules onto the surface and the creation of a corrosion protection coating [7]. Therefore, the electronic structure of organic inhibitors has a significant impact on how effective they are in preventing metal corrosion. The selection of effective inhibitors has mostly been based on an empirical understanding of their mechanisms of action, macroscopically physicochemical features, and capacity to donate electrons. Thus, molecular structure, hydrophobicity, electron density at donor atoms, dispensability, and solubility are the most important factors to consider when choosing an inhibitor.

While the experimental determination of inhibition efficiency is a critical step in identifying effective molecules in corrosion chemistry, computational techniques such as density functional theory (DFT), qualitative structural activities relationship modeling, and others are becoming increasingly more popular for identifying likely effective molecules in a timely and efficient manner. For instance, quantum chemical computations are a useful tool for investigating and understanding the electronic structures and reaction mechanisms of organic corrosion inhibitors interpreting the experimental results, resolving chemical ambiguities, and predicting molecular parameters that are closely associated with the corrosion inhibition property of the chemical compound. Qualitative structural activities relationship is commonly used to relate the quantum descriptors with experimental inhibition efficiencies as well as, developing models for similar molecules with unknown inhibition efficiency. In essence, it is used to investigate the structure-activity relationship of molecules. The most promising technique used to ascertain the electronic structure of matter at the moment is density functional theory, commonly known as chemical]reactivity theory [8].

In continuation of our work on the investigation and theoretical prediction of organic molecules as inhibitors of corrosion [9], this research work investigates and predicts the corrosion of thiosemicarbazide derivatives (Figure 1) in the corrosion inhibition of aluminum from the perspective of molecular modeling and quantitative-structural-activity relationships. Thiosemicarbazides are Schiff bases- organic compounds formed as a result of condensation of a carbonyl and an amine and according to literature, they have shown to be potential inhibitors. Several authors [10-12] have observed that the presence cyano group and other heteroatoms such as oxygen and sulfur atoms make Schiff bases effective inhibitors in metallic corrosion in alkaline and acidic conditions [13]. The nitrogen (N) atom's lone pair of electrons and planarity (π) of the Schiff Bases are also essential structural properties that influence their adsorption on metal surfaces [14]. These molecules also are useful intermediates in the production of pharmaceutical and bioactive materials, and they are widely utilized in medicinal chemistry. The corrosion inhibition of thiosemicarbazide derivatives studied has been experimentally investigated by Fouda et al. [15]. This work presents a theoretical investigation on molecular and electronic properties of thiosemicarbazide derivatives with the aim of determining the relationship between the structural properties of thiosemicarbazide derivatives and their inhibition efficiency. The model derived from the QSAR relationships might be useful in predicting other derivatives of thiosemicarbazide theoretically. The quantum parameters like hardness (η), dipole moment (μ), molecular orbital energies (E_{HOMO} and E_{LUMO}), the charge distribution, total energy (E_{total}), a fraction of electrons (ΔN) transfer and electronegativity (χ) values were estimated and correlated with inhibition efficiencies (% IE).

2. Methodology

2.1. Molecular modeling

Molecular modeling of six (6) thiosemicarbazides (Figure 1) were performed using the SPARTAN 14 program package [16]. Density Functional Theory (DFT) with the B3LYP exchange functional [17-18] at 6-311G* basis set was utilized to optimize geometrical structures. During optimization, dihedral and bond angles, as well as all bond lengths, were free of constraints while real vibrational frequencies were ensured for the entire geometries. The Fukui functions of thiosemicarbazides derivatives were evaluated using electron populations for their neutral and ionic neutral species.

When an inhibitor is in contact with aluminum (Al), electrons flow from the inhibitor which has lower electronegativity to the metal which has higher electronegativity until the chemical potentials are equal [19]. Equation 1, as a first approximation, gives the proportion of electrons transferred (ΔN).

$$\Delta N = \frac{\chi_{Al} - \chi_{inh}}{2(\eta_{Al} + \eta_{inh})} \tag{1}$$

where χ_{inh} *and* χ_{Al} symbolize absolute electronegativities of organic inhibitor and aluminum (Al) respectively while η_{inh} and η_{Al} symbolize absolute hardness of the organic inhibitor and Aluminum (Al) respectively.

These parameters are related to electron affinity (A) and ionization potential (I), both of which can be used to predict chemical behavior as shown in equations 2 to 3 [20].

$$\eta = \frac{IP - EA}{2} \tag{2}$$

$$\chi = -\mu = \frac{IP + EA}{2} \tag{3}$$

Theoretically, Aluminum (Al) has absolute electronegativity(χ_{Al}) and hardness (η_{Al}) values of 3.23 eV/mole and 0 $eV/mole$) respectively[19, 21].

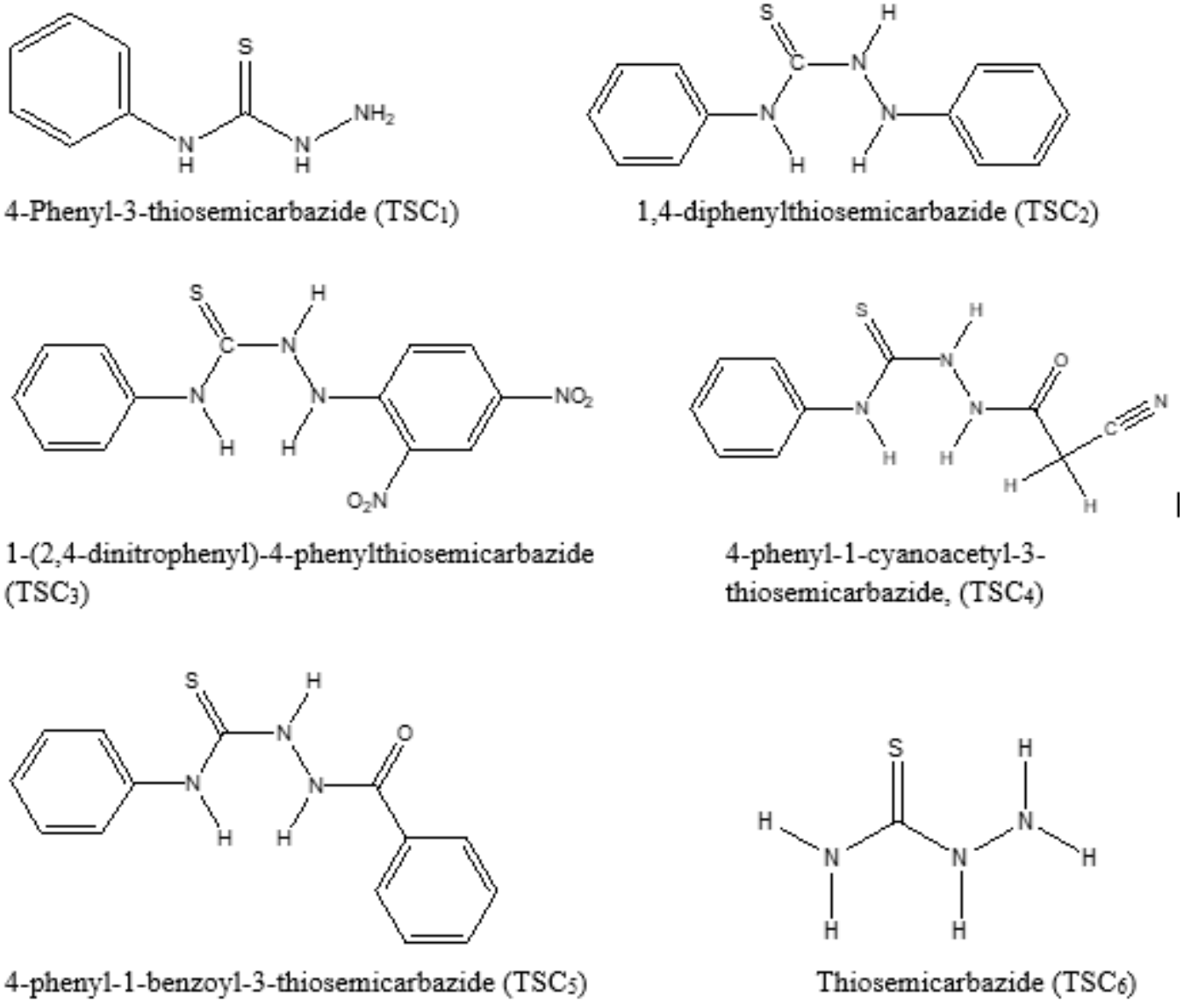

Figure 1. Structures of the studied thiosemicarbazide derivatives

Meanwhile, the inverse of hardness, softness, is likewise a quantum parameter that may be determined using equation 4 [22].

$$S = \frac{1}{\eta} \tag{4}$$

Koopman's theorem [18] asserts that electron affinity (A) and ionization potential (I) are also related to the molecular orbital energies (E_{HOMO} and E_{LUMO}) of an inhibitor, as shown in Eqs. (5) and (6)

$$IP = -E_{HOMO} \tag{5}$$

$$EA = -E_{LUMO} \tag{6}$$

Equation (7) was used to determine the electrophilicity index which evaluates the stabilization energy when charges are transferred to a system from an environment [23]

$$\omega = \frac{\mu^2}{4\eta} \tag{7}$$

Whenever the values of chemical potential (μ) and electrophilicity index (ω) are low, it indicates that inhibitory compounds are more reactive nucleophiles, whereas high values indicate that they are more reactive electrophiles

Furthermore, the Local reactivity index describes the reactivity of a specific chemical atom in relation to an organic inhibitor's adherence to a certain surface of a metal. Also, using the computation of the determinate variance, the difference in electron density for a nucleophile $f^{+}_{(r)}$ and electrophile $f^{-}_{(r)}$ as the Funki functions may be computed [24].

$$f^{+}_{(r)} = qk^{N+1}_{(r)} - qk^{N}_{(r)} \quad \text{(for nucleophilic attack)} \tag{8}$$

$$f^{-}_{(r)}fk == qk^{N}_{(r)} - qk^{N-1}_{(r)} \quad \text{(for electrophilic attack)} \qquad (9)$$

Where $qk^{N+1}_{(r)}$, $qk^{N}_{(r)}$ $qk^{N-1}_{(r)}$ are the electronic densities of anionic, neutral, and cationic species respectively.

2.2. Quantitative structural activity relationship (QSAR)

QSAR was developed to explain the structure-activity relationship of molecular descriptors based on quantum chemical calculations of six thiosemicarbazide derivatives as corrosion inhibitors. The quality of a model in this type of analysis is determined by the model's ability to fit and predict accurately. This method looks for a relationship in the form of an equation that connects molecular descriptors to the inhibition efficiency determined experimentally. Lukovits' linear equation is commonly employed in corrosion inhibitor research to allow the correlation of quantum molecular descriptors with experimental inhibitory efficacy [25] as shown in equation 10 below

$$\%\text{IE} = \acute{\alpha} + \boldsymbol{\beta}_1 X_1 \ + \boldsymbol{\beta}_2 X_2 \ldots\ldots\ldots \boldsymbol{\beta}_n X_n \qquad (10)$$

X_1, X_2.... X_n indicate are quantum chemical descriptors of the modelled inhibitors while $\acute{\alpha}$ and β are the regression coefficients calculated from regression analysis.

2.3. Test of model

The model developed was statistically validated by utilizing the squared fitting factor (R^2), adjusted fitting factor (R^2_a), cross-validation ($CV.R^2$) and variation ratio (F).

The adjusted fitting factor(R^2_a), is defined as follows:

$$R^2_a = \frac{N-1)\ X\ R^2 - P}{N - P - 1} \qquad (11)$$

Where N represents the number of observations (study molecules) and p is the number of descriptors, cross-validation ($CV.R^2$) is a mathematical approach for ensuring the reliability of the QSAR model as given in equation 12.

$$CV.R^2 = \frac{\sum (Y_{obs} - Y_{cal})^2}{\sum \left(Y_{obs} - \hat{Y}_{obs}\right)^2} \qquad (12)$$

The variance ratio (F) was also used to determine the overall significance of the regression coefficients [26]. As shown in equation 13 below, it is defined as the ratio of the regression mean square to deviations mean square:

$$F = \frac{\frac{\sum \left(Y_{cal} - \hat{Y}_{obs}\right)^2}{p}}{\frac{\sum (Y_{obs} - Y_{cal})^2}{N-P-1}} \qquad (13)$$

At $p < 0.05$, a model's estimated F value should be significant; consequently, the F value for the overall significance of the regression coefficients should be high [27].

3. Results and Discussion

3.1. Quantum descriptors of inhibitors

The optimized structures of the six thiosemicarbazide derivatives using DFT/B3LYP/6-311 G* are displayed in Figure 2. Suggested quantum descriptors that may be responsible for the effective inhibition of the investigated molecules are; Energy band gap (ΔE), E_{HOMO}, E_{LUMO}, dipole moment (DM), polarizability, ovality, Log P, Affinity (EA), global electrophilicity (ω), Ionization Potential (IP), softness (S), electronegativity (χ), chemical hardness (μ), total energy, electron transfer (ΔN) and solvation energy (E_{solv}), (Table 1).

The E_{HOMO} is associated with the electron donor ability of an inhibitor. The high or elevated E_{HOMO} of inhibitors indicates a higher tendency to donate electrons to the corresponding lower molecular orbital of the metal. This improves the adsorption capacity and inhibition efficiency of inhibitors to the surface of a metal. Therefore, the effectiveness of an inhibitor can be improved by enhancing the transferring process. In Table 1, it is clear that the E_{HOMO} value for the six thiosemicarbazide derivatives molecules (TSC_{1-6}) corresponds to $TSC_5 > TSC_2 > TSC_1 > TSC_6 > TSC_4 > TSC_3$. The highest E_{HOMO} (-5.54 eV) for TSC_5, is indicated as the best electron-donating inhibitor to the empty d-orbital of the metal. Organic inhibitors, on the other hand, not only donate electrons to the metal's empty d-orbitals but also accept electrons from the metal's d-orbital.

Thus E_{LUMO} shows the capability of an inhibitor to accept electrons from the metal which would definitely improve the inhibition effect on the surface of the metal. The E_{LUMO} for TSC_{1-6} follows the sequence: $TSC_6 > TSC_2 > TSC_1 > TSC_4 > TSC_5 > TSC_3$, indicating that the TSC_3 has an improved propensity to accept electrons from the surface of a metal. The evaluation of the distribution of electron density in molecular orbitals (Fig 3) indicates that electrons are localized on the atoms of both aromatic rings of the six studied molecules.

The energy difference which is also known as bandgap energy (ΔE) which is the difference in E_{LUMO} and E_{HOMO} of a molecule, relates the inhibitor's reactivity to adsorption on the metal surface. Decreasing the ΔE value of inhibitors increases the reactivity between the metal and inhibiting molecule which consequently increases the binding capacity at the surface of the metal. This increase in binding capacity can result in an increase in the inhibitory efficiency (%IE) of the inhibitor since the energy required to remove the electron from the highest occupied molecular orbital will be less. The addition of $-C_6H_5$, $-C_6H_3(NO_2)_2$ $-COCH_2CN$, and $-COC_6H_5$ substituents to semicarbazide (TSC_6) to give their respective derivatives (TSC_{1-5}) greatly have an effect band gap. A very low band gap of 4.42 eV was recorded for TSC_2 when the phenyl group was attached to TSC_1 and a further reduction to 2.94 eV in TSC_3 when the NO_2 substituent was attached to the attached phenyl group could be a result of the destabilization of the highest unoccupied molecular orbital (LUMO) to lower energy level. The presence of a positive charge on the Nitrogen atom in NO_2 deactivates the aromatic system and "sucks" electron density from the aromatic system by positive inductive effect and influences the resonance stabilization of the system [28].

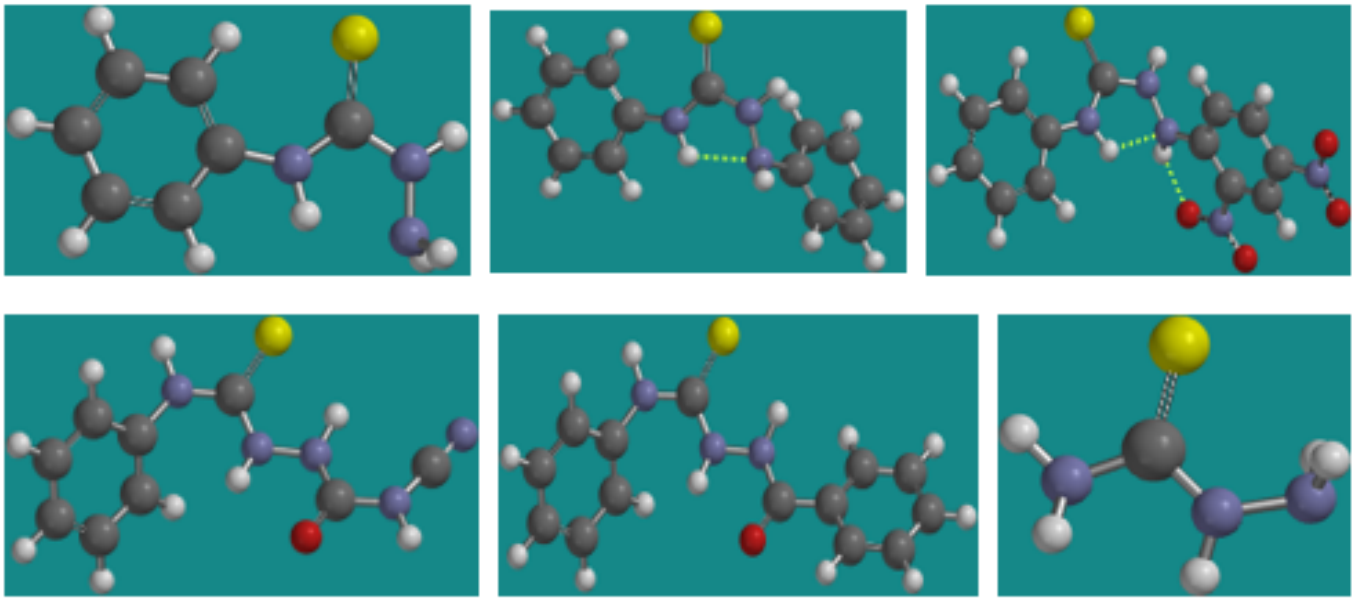

Figure 2. Optimized molecular structures of thiosemicarbazide derivatives using DFT/B3LYP/6-311G*

Table 1. Quantum chemical parameters of some of the thiosemicarbazide derivatives using DFT/B3LYP/6-31 1G* method

Quantum parameters	TSC 1	TSC2	TSC 3	TSC 4	TSC 5	TSC 6
E_{HOMO} (eV)	-5.68	-5.56	-6.22	-6.07	-5.54	-5.76
E_{LUMO} (eV)	-0.63	-1.14	-3.28	-1.13	-1.36	-0.20
IP (eV)	5.68	5.56	6.22	6.17	5.94	5.76
EA (eV)	0.63	0.53	3.28	1.13	1.36	0.20
Hardness (η)	2.53	2.221	1.47	2.52	2.09	2.78
Softness (S)	0.404	0.397	0.680	0.396	0.436	0.35
Electronegativity (χ)	3.155	3.35	4.75	3.65	3.45	2.98
Electron transfer (ΔN) e^-	0.0145	-0.027	-0.517	-0.083	-0.053	0.045
$E_{Back-donation}$	-0.788	-0.838	-1.18	-0.91	-0.86	-0.75
Electrophilicity index (ω)D2/eV	1.967	2.526	7.674	2.643	2.85	1.597
Energy difference (ΔE) eV	5.05	4.42	2.94	5.04	4.18	5.56
polarizability (α)	53.50	60.54	64.44	57.93	62.25	46.43
Log p	0.33	1.11	0.37	0.34	1.14	-0.67
Area (A) cm^3	189.62	273.01	322.49	248.90	294.11	108.60
Volume (V) cm^3	164.20	250.67	292.94	218.81	270.74	78.11
ovality	1.31	1.42	1.51	1.42	1.45	1.22
Solvation energy (E_{sol}) kJ/mol	-58.13	-41.67	-40.08	-52.90	-46.05	-67.65
Dipole moment (debye)	5.65	5.02	2.13	6.07	2.06	4.07
Molecular weight (amu)	167236	243.334	333.328	235.271	271.244	91.138
PSA	49.083	32.635	104.823	69.777	42.974	66.43
Exp. IE	27.4	94.3	92.8	60.8	95.5	27

Polar surface area(PSA), ionization potential (IA), Electron Affinity (EA)

The ΔE value shown in Table 1 indicates $TSC_3 < TSC_5 < TSC_2 < TSC_4 < TSC_1 < TSC_6$, suggesting that TSC_3 TSC_5 and TSC_2 have a low energy gap, higher reactivity, and therefore, better performance than other molecules. However, the higher experimental inhibition efficiency reported for TSC_3 with the lowest band gap could be a result of an external factor acting on the inhibitor. In an acidic solution, the hydrogen evolved can cause a reduction of the nitro group in TSC_3 which can aid the desorption of TSC_3 thus making it a less effective corrosion inhibitor than TSC_2 and TSC_5

Absolute hardness, electronegativity, and softness are indicators of reactivity that are derived from electronic energy (E) with respect to the number of electrons (N) at a constant external potential t(r) [29]. The absolute hardness and softness reactivity descriptors are associated with the description of soft and hard solutions through the acid and base theory [30-31]

established that the hardness of all atoms in a molecule is actually equalized, and molecular hardness equals the geometric mean of component atoms' chemical hardness [32]. The transfer of electrons between chemical species occurs in every reaction and in contrast to hard molecules, soft molecules are affected by charge transfer. The Principle of Maximum Hardness (PMH) [33-34] states that chemical stability is directly linked to chemical hardness and that molecules that are hard are more stable and less reactive. As a result, the chemical hardness of a molecule denotes the resistance of the electron cloud of ions, atoms or molecules to polarization or deformation resulting from chemical reaction perturbations. The chemical hardness of a reaction also gives vital information for predicting the reaction mechanism and estimating the products generated throughout the reaction [35]. The values of absolute hardness for TSC_{1-6} follows the sequence: $TSC_3 < TSC_5 < TSC_2 \approx TSC_4 < TSC_1 < TSC_6$. This result shows that TSC_2, TSC_3 and TSC_5 have a low hardness value of 1.47, 2.09, and 2.51 eV respectively, compared to the other three studied derivatives. Hence, these three molecules are less stable and more reactive. Derivatives with low hardness values show low bandgap and hence the high inhibition efficiency. This corresponds to the widely held idea that soft molecules should have a small energy gap whereas hard molecules should have a high energy gap. The softness values of the studied molecules using DFT is as follows the sequence: $TSC_3 < TSC_5 < TSC_2 < TSC_4 < TSC_1 < TSC_6$. This trend shows that the first three soft thiosemicarbazide derivatives (TSC_2, TSC_3 and TSC_5) have experimental inhibition efficiencies that are more than 90%. Hence low global hardness value (that is, the high global softness value) is likely to show high inhibition efficiency. The experimental inhibitory efficiency of the investigated compounds agrees with this trend.

The tendency of an atom in a molecule to attract shared pair of electrons to itself is known as electronegativity and it is a key concept to understanding the nature of chemical interactions [34]. The electronegativities of atoms in a molecule are equilibrated during molecule formation and molecular electronegativity is the geometric mean of the atoms' electronegativities [34]. The electronegativity values of studied molecules TSC_{1-6} (Table 1) are: $TSC_6 < TSC_1 < TSC_2 < TSC_5 < TSC_3 < TSC_4$.

The dipole moment (DM) is the first derivative of the energy with respect to an applied field [36] electronic parameter resulting from the unequal distribution of charges on various atoms in a molecule. It measures the polarity of a polar covalent bond, predicts the direction of the corrosion inhibition process, and gives information about the distribution of electrons in the molecules [36-38]. The total dipole moment, on the other hand, simply represents a molecule's global polarity.

The overall molecular dipole moment can be estimated as the vector sum of individual bond dipole moments for a whole molecule. A high dipole moment may increase the adsorption between the metal surface and the molecules of inhibitors [39]. This statement is consistent with TSC_3. However, TSC_1 and TSC_4 with high dipole moment (5.65 and 6.07 Debye respectively) have poor inhibition efficiency, while TSC_2 and TSC_5 with low dipole moment, have a high inhibition efficiency. These results show that there is inconsistency with the use of dipole moment predicting the direction of a corrosion inhibition reaction.

In the examined compounds, our theoretical results confirmed that there is no substantial link between inhibitory effectiveness and dipole moment. The electrostatic potential may be used to deduce the dipole's orientation (right panels of Fig. 3). The colors represent the electrostatic potential value. Colors lean toward red represent places with negative potential (where a positive charge is most likely to be attracted), while colors that lean toward blue represent areas of positive potential (where a positive charge is least likely to be attracted). The region of highest electron density is found around the sulphur atom and around the nitrogen atom.

Log P is responsible for the hydrophobicity (property of a molecule to repel water) of a molecule [40-41]. In corrosion studies, hydrophobicity can be related to the process at which oxide/hydroxide layers which retards the corrosion process are formed on the surface of the metal. Hydrophobicity will increase when the solubility of the molecule in water decreases [42]. The results obtained for log P showed that $TSC_5 > TSC_2 > TSC_3 > TSC_4 > TSC_1 > TSC_6$. It was also found that the values of log P are closely related to the corrosion inhibition efficiencies of the investigated derivatives.

The effective surface coverage and molecular size of the inhibitor on the surface of metal are determined by using molecular weight and volume quantum parameters. These parameters determine how well a molecule can be adsorbed atop and cover a metal surface, thereby isolating it from the corroding environment. The molecular volume and weight for the six studied molecules increases in the following order: $TSC_3 > TSC_5 > TSC_2 > TSC_4 > TSC_1 > TSC_6$. The presence of the phenyl group increases the molecular size of TSC_1, would lead to a larger surface coverage that TSC_6 on the aluminum. Also, TSC_2 has two phenyl groups and consequently more effective than TSC1. Hence as the value of this parameter increases, so do the molecule's corrosion inhibition potential increases

The fraction of electrons transferred (ΔN) is the number of electrons transferred from the inhibiting molecule to the surface of the metal. It also presents the inhibitor's ability to transfer electrons. When the electron-donating capacity of an inhibitor is improved, its inhibitory efficiency on the surface of metal also improves. Similarly, the efficiency of an inhibitor increases on the face of metal as the number of electron transfers increases. The number of electrons transferred (ΔN) in an organic inhibitor should be less than 3.6 (electrons) for it to be regarded effective in increasing the corrosion inhibition efficiency, but if the ΔN is greater than 3.6 (electrons) the inhibition efficiency decreases [25]. Molecules with higher electron transfer value, has a greater tendency to donate electrons to molecules that accept electrons. This implies that inhibiting molecules with higher ΔN have greater tendency to adsorb on the surface of the metal which consequently increases their inhibition efficiencies [25]. The ΔN values for the six studied molecules range from -0.517- 0.45 e^-. For the molecules TSC_{1-6}, the largest proportion of electron transferred (ΔN) is

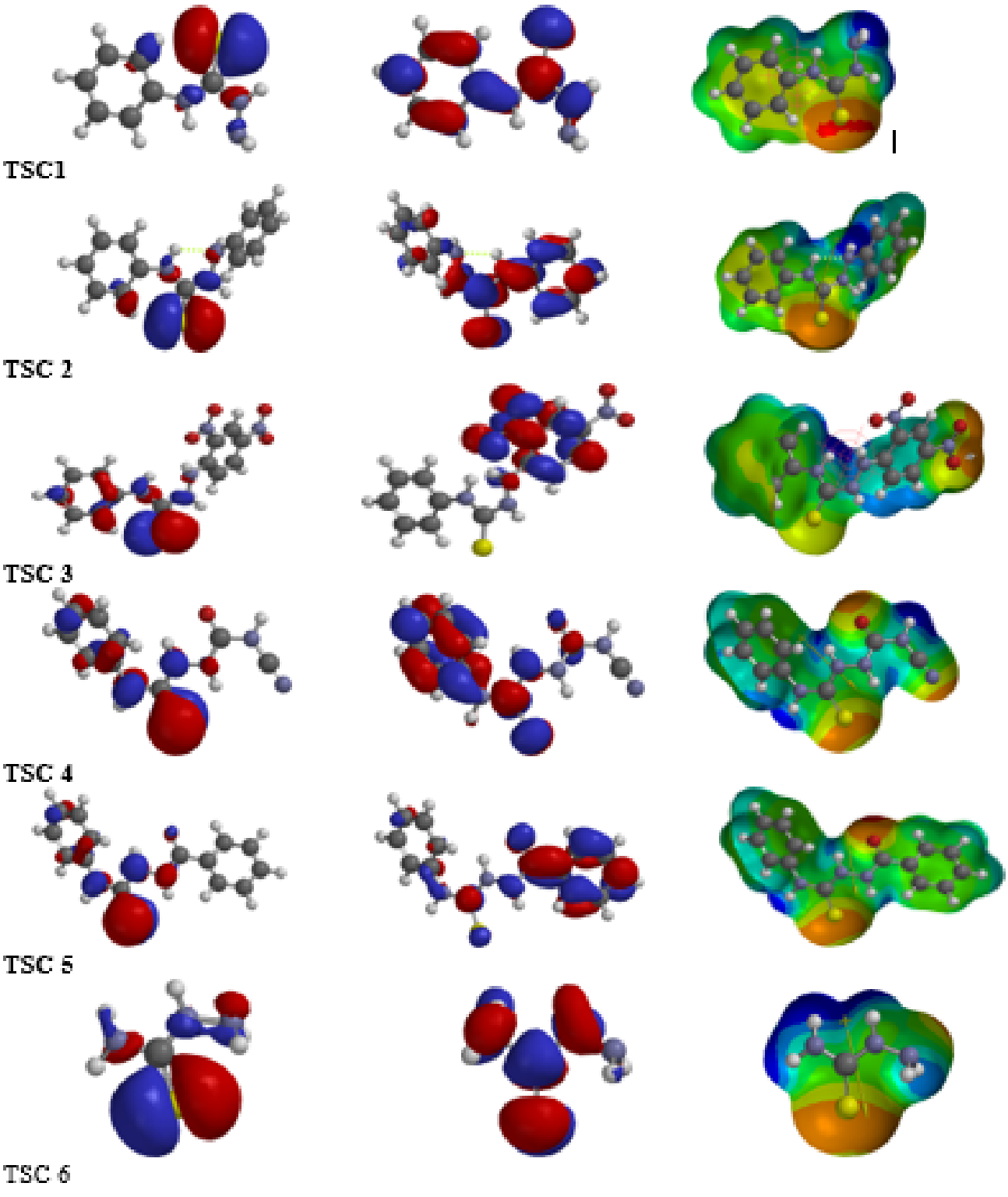

Figure 3. Molecule orbital density distribution of studied thiosemicarbazides: HOMO (left), LUMO (middle) and electrostatic potential (right)

associated with molecule TSC_3, while the lowest proportion is associated with TSC_6 which has the lowest inhibition efficiency. ΔN for molecules TSC_{1-6} increases in the following order: $TSC_3 > TSC_4 > TSC_5 > TSC_2 > TSC_1 > TSC_6$. The results indicate that there is no correlation between the trend in the ΔN values of these studied compounds and the trend in the experimentally determined inhibition efficiency. The ΔN values are strongly influenced by the molecular structure and

substituent groups attached to the thiosemicarbazide skeletal ring. This result demonstrates that the studied thiosemicarbazide derivatives are electron-donating molecules while the aluminum surface could be an electron-accepting molecule.

It's crucial to evaluate the circumstance involving a molecule that will acquire a particular amount of charge at one center and then back-donate the same amount of charge through the same or a different center. In a simple model of charge transfer for donation and back donation of charges [42], an electronic back donation process can be a result of the interaction between the inhibiting molecule and the surface of a metal. Though, it is necessary to note that these values do not predict the occurrence of a back donation process. Back-donation charges for the studied molecules are less than zero (-0.75 to -1.18 e) indicating that the charges transferred to the molecules, accompanied by a back-donation from the molecule, are energetically favoured since $\eta > 0$ and $\Delta E_{back-donation} < 0$. Therefore, TSC_3 and TSC_4 could be more energetically favoured than TSC_1 and TSC_2. The result is consistent with the concept that states that if both charge transfer (*i.e.* to the molecule and back-donation processes from the molecule) occurs, the change in energy is directly proportional to the hardness of the molecule in equation 3.

The global electrophilicity index (ω) gives information on the nucleophilicity and electrophilicity nature of organic inhibitors. An inhibitor with a high electrophilicity index (ω) value indicates a high tendency to act as an electrophile and conversely a low electrophilicity index (ω) value indicates a high tendency to act as a nucleophile. The electrophilicity values (Table 1) show that TSC_3 has the highest value and as a result, the largest ability to receive electrons from the metal thereby increasing the adsorption capacity of the TSC_3 on the surface of the metal. The electrophilicity values show the following sequence: $TSC_3 > TSC_5 > TSC_4 > TSC_2 > TSC_1 > TSC_6$. The inhibitors function as Lewis bases in a corroding system, whereas the metal acts as a Lewis acid.

The distribution of charges in the chemical structure of organic inhibitors influences adsorption. The charge distribution on a molecule might reasonably be taken as an indication for locating the positions of interaction between the inhibitor and the metal surface. Charge distribution in the studied molecules is estimated using Mulliken population density [9, 43]. It is a way of estimating inhibitors' adsorption centers and consequently determining the site that corresponds to a molecular center that accepts the charge as well as a molecular center that will donate back charges via the same center or another center. Moreover, In the physisorption model, electrostatic attraction is expected between the metal surface and inhibiting molecules. The charges on heteroatoms of inhibitors can apparently be utilized as an index to account for physical adsorption. According to this hypothesis, the molecule with the highest atomic charge on a heteroatom will have a greater potential to physically adsorb on the metal surface [44]. The average Mulliken charges for heteroatoms present in each of the studied thiosemicarbazides (denoted as Heteroatom) are -3.16, -2.57, -2.18, -1.768, -1.75, and -0.57, for TSC_4, TSC_3, TSC_1, TSC_6, TSC_2, and TSC_5, inhibitors respectively. Inhibitors with more negatively charged heteroatom will adsorb more on the surface of the metal through the donor-acceptor reaction [45]. Therefore, a higher electron density on TSC_4 and TSC_3 and TSC_1 heteroatoms would promote its physical adsorption on the surface of the metal.

Condensed Fukui functions are often used to investigate local reactivity in inhibitors. The Fukui function reveals the location in a chemical compound where electrophilic(f_k^-), nucleophilic (f_k^+) and radical reactions are most likely to occur. f_k^+ measures the change in density when the inhibiting molecule gains electrons which is related to the reactivity with respect to nucleophilic attack. Conversely, f_k^- is related to the reactivity when the molecule losses electrons which is reactivity related to electrophilic attack. Atoms with larger Fukui function values are better reactive atomic centers than lower values in a given molecule. The Fukui indices (f_k^+ and f_k^-) of the studied molecules calculated from Mulliken charge population analysis are given in Table 2 for TSC_1, TSC_2, TSC_3, TSC_4, TSC_5, and TSC_6, respectively. The highest value of f_k^- for the non-hydrogen atoms was found on C7 (0.06) of TSC_1, C7 (0.96) and N (0.96), for TSC_2, C7 (0.082), C12 (0.065) and O4 (0.0854) for TSC_3, C8 (0.05) and C7 (0.047) for TSC4, C12 (0.037), C_7 (0.065) and O1 (0.063) for TSC_5 and C (0.042) for TSC_6 which represents the most probable centers for electrophilic attack. However, the highest values for f_k^+ for non-hydrogen atoms are found on S1 (0.323) and N1 (0.051) for TSC_1, S1 (0.262) and N1 (0.048) for TSC_2, S1 (0.321) and N1 (0.057) for TSC3, S1 (0.386) and N1 (0.065) for TSC4, S1 (0.195), N1 (0.064), N2 (0.044) for TSC_5, S1 (0.233) and N (0.311) for TSC_6. These represent the most probable centers for nucleophilic attack in the molecules.

3.2. *Quantitative Structure-Activity Relationships (QSARs) modeling*

Experimentally, the potentiodynamic polarization method has been used to evaluate the inhibitory efficiency (IE) of thiosemicarbazide derivatives (TSC_{1--6}) (15). However, theoretically calculated inhibition efficiencies (IE%) of studied thiosemicarbazide derivatives (TSC_{1-6}) were predicted using the QSARs model (equation 14) developed via linear regression of molecular descriptors (Table 1). The experimentally measured inhibitory efficiency (IE percent) against steel served as dependent variables, whereas the appropriate molecular descriptors as determined by Pearson's matrix (Figure 4) served as independent variables. These selected descriptors were used to build a linear QSAR model to understand how linear regression equations might explain structural key points corresponding to differential behavior in chemical descriptors against corrosion.

As indicated in equation 14, the molecular descriptors solvation energy (E_{solv}), softness (S) electronegativity, and dipole moment define the corrosion inhibition of the thiosemicarbazide derivatives.

$$\%IE = 262 - 117 * softness + 7.81 * Electronegativity + 2.90 * E_{solv} - 4.87 * Dipole \quad (14)$$

The acceptability of the quality of the model developed from the QSAR investigation is determined by its predictabilities and

Table 2. Fukui indices for the atoms of the studied thiosemicarbazide derivatives

	TSC 1			TSC 2			TSC 3			TSC 4			TSC 5			TSC 6	
Atoms	f_k^-	f_k^+	*atoms*	f_k^-	f_k^+	*atom*	f_k^-	f_k^+	*atom*	f_k^-	f_k^+	*atoms*	f_k^-	f_k^+	*atoms*	f_k^-	f_k^+
CI	0.026	0.041	CI	0.067	0.027	CI	0.001	0.029	CI	0.016	0.023	CI	0.007	0.014	N1	-0.01	0.051
H2	0.032	0.026	H2	0.024	0.026	H2	0.007	0.024	H2	0.045	0.042	H2	0.018	0.031	H1	0.036	0.042
C2	0.008	0.014	C2	0.006	0.009	C2	0.003	0.011	C2	0.007	0.01	C2	0.002	0.009	C7	0.067	-0.024
H4	0.071	0.069	H4	0.055	0.059	H4	0.022	0.063	H4	0.065	0.06	H4	0.038	0.052	S1	0.026	0.323
C3	0.048	0.04	C3	0.036	0.038	C3	0.006	0.044	C3	0.045	0.039	C3	0.027	0.032	N2	0.031	0.019
H3	0.089	0.08	H3	0.067	0.07	H3	0.024	0.076	H3	0.08	0.069	H3	0.051	0.062	H11	0.049	0.041
C4	0.006	0.014	C4	0.004	0.009	C4	0.002	0.011	C4	0.006	0.009	C4	0.003	0.009	N3	-0.006	-0.003
H6	0.076	0.073	H6	0.056	0.06	H6	0.016	0.066	H6	0.07	0.062	H6	0.046	0.056	H7	0.052	0.04
C5	0.017	0.033	C5	0.014	0.025	C5	0.001	0.028	C5	0.023	0.027	C5	0.013	0.023			
H5	0.068	0.067	H5	0.042	0.051	H5	-0.014	0.062	H5	0.061	0.052	H5	0.037	0.048			
C6	0.039	0.021	C6	0.023	0.015	C6	0	0.02	C6	0.037	0.001	C6	0.014	0			
N1	-0.01	0.051	N1	-0.005	0.048	N1	-0.005	0.057	N1	-0.007	0.069	N1	0.001	0.064			
H1	0.036	0.042	H1	0.024	0.031	H1	-0.013	0.04	H1	0.043	0.041	H1	0.03	0.042			
C7	0.067	-0.024	C7	0.096	-0.029	C7	0.082	-0.029	C7	0.047	-0.042	C7	0.065	-0.031			
S1	0.026	0.323	S1	0.092	0.262	S1	0.042	0.321	S1	0.028	0.286	S1	0.042	0.295			
N2	0.031	0.019	N2	0.022	0.02	N2	-0.022	0.026	N2	0.019	0.03	N2	0.003	0.044			
H11	0.049	0.041	H11	0.037	0.027	H11	0.117	-0.125	H11	0.018	0.018	H11	0.265	0.023			
N3	-0.006	-0.003	N3	0.094	-0.836	N3	0.016	-0.02	N3	-0.003	-0.005	N3	0.007	0.049			
H7	0.052	0.04	H7	0.03	0.031	H7	0.026	0.011	H7	0.019	0.011	H7	0.011	0.026			
			C8	0.004	0.004	C8	0.067	-0.005	C8	0.05	0.016	C8	0.065	0.014			
			C9	-0.388	0.01	C9	-0.029	-0.451	C9	0.025	0.005	C9	0.009	0.001			
			C10	0.031	0.006	C10	-0.045	0.01	N4	0.001	0.007	C10	0.023	0.011			
			C11	0.079	-0.15	C11	0.003	0.009	N5	0.042	0.026	C11	0.005	0.008			
			C12	0.009	0.006	C12	0.065	0.009	O1	0.058	0.024	C12	0.037	0.017			
			C13	0.032	0.012	C13	0.012	-0.002				C13	0.003	0.006			
						N4	0.052	0.005				O1	0.043	0.093			
						N5	0.024	0.002				C14	0.025	0.008			
						O1	0.133	0.03									
						O2	0.123	0									
						O3	0.071	0.019									
						O4	0.854	-0.761									

fitting capabilities (9). The developed QSAR model in equation 14, reproduced the experimental %IE (R^2 = 0.9982) with deviation ranging between 0.03 and 0.06 while the standard error of residuals is 0.116212. Table 3 compares the predicted corrosion inhibition efficiency (% IE) of molecules 1 through 6 to their experimental %IE. Figure 5 depicts a graph of experimen-

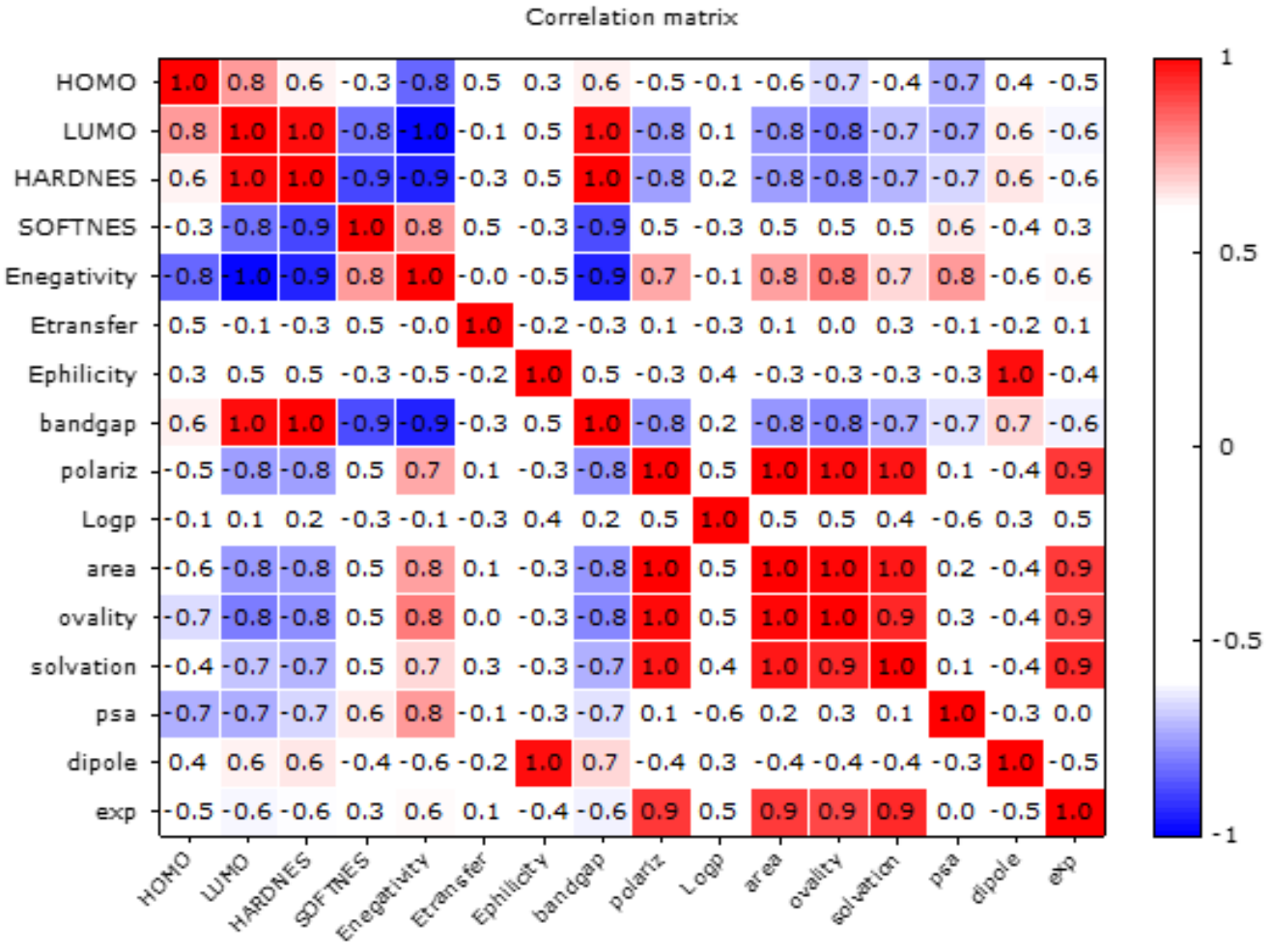

Figure 4. Generated Pearson's matrix

Table 3. Experimental and Predicted inhibition efficiencies of thiosemicarbazide derivatives

Molecules	Experimental inhibition efficiency	Predicted inhibition efficiency	Residual
TSC_1	27.4000	27.4352	-0.0352155
TSC_2	94.3000	94.2488	0.0512029
TSC_3	92.8000	92.7691	0.0308704
TSC_4	60.8000	60.8311	-0.0311049
TSC_5	95.5000	95.5642	-0.0642269
TSC_6	27.0000	26.9515	0.0484739

tal corrosion inhibition efficiency (% IE) vs predicted corrosion inhibition efficiencies (% IE) to illustrate the relationship between the two. The developed model was quite resilient in predicting good experimental values, Therefore, the theoretical percentage inhibition efficiency for the studied compounds follows: $TSC_2 > TSC_6 > TSC_3 > TSC_5 > TSC_4 > TSC_1$.

The model was also statistically validated using the squared fitting factor (R^2), adjusted fitting factor (R_a^2), cross-validation (CV. R^2), and variation ratio (F). The estimated R^2 (0.9982) revealed a reasonable fitness as well as the model's efficiency, as shown in equation 14. The calculated CV.R^2 (0.9342) is greater than 0.5 (standard) while the R_a^2 (0.9143) is greater than 0.6. These results show that the model is statistically reliable and acceptable and have strong external predictability.

4. Conclusion

The quantum chemical descriptors of thiosemicarbazide derivatives were investigated in order to elucidate their electronic structure, reactivity, and predict their potential for corrosion inhibition using a computational approach. Through DFT/B3LYP/6-311G* computational method, a relationship between quantum

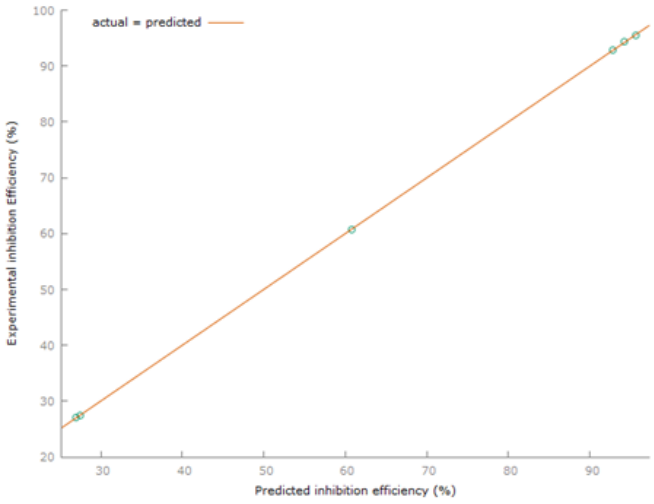

Figure 5. Graphical representation of the experimental and predicted inhibition efficiency (%) of the studied thiosemicarbazise derivatives

descriptors of six thiosemicarbazide derivatives and their effectiveness in preventing corrosion was established. The correlations were found to be effective in developing thiosemicarbazide inhibitors with appropriate substituents capable of donating electrons to the metal's surface. Because of their high E_{HOMO}, ΔN, and low ΔE values, TSC_2, TSC_3 and TSC_5 are projected to have the best inhibition efficiency, allowing for efficient electron transfer and hence a higher performance as corrosion inhibitors. This theoretical work has an excellent correlation with experimental corrosion inhibition efficiency, indicating that the approach used in this study is reliable. The additional NO_2 and CN functional groups present in TSC_3 and TSC_4 respectively may give insight into the preferred moieties to look for when designing corrosion inhibitors while the correlations and model developed might aid in the design of novel thiosemicarbazide inhibitors with appropriate substituents capable of donating electrons to a metal's surface.

References

[1] K. K. Adamaa & I. B. Onyeachub ,"The corrosion characteristics of SS316L stainless steel in a typical acid cleaning solution and its inhibition by1-benzylimidazole: Weight loss, electrochemical and SEM characterizations", Journal of the Nigerian Society of Physical Sciences **4** (2022) 214.

[2] P. Vijayan & M. Al-Maadeed, "Self-Repairing Composites for Corrosion Protection: A Review on Recent Strategies and Evaluation Methods", Materials **12** (2019) 2754. https://doi.org/10.3390/ma12172754

[3] M. Finsgar & J. Jackson, "Application of corrosion inhibitors for steels in acidic media for the oil and gas industry: A review", Corrosion Science **86** (2014) 17.

[4] C. G. Dariva & A. F. Galio "Corrosion Inhibitors - Principles, Mechanisms and Applications, in Developments in Corrosion Protection", InTech (2014) 365.

[5] Y. Meng, W. Ning, B. Xu, W. Yang, K. Zhang, Y. Chen, et al. "Inhibition of mild steel corrosion in hydrochloric acid using two novel pyridine Schiff base derivatives: A comparative study of experimental and theoretical results", RSC Advances **7** (2017) 43014.

[6] O. Krim, A. Elidrissi, B. Hammouti, A. Ouslim & M. Benkaddour, "Synthesis, characterization, and comparative study of pyridine derivatives as corrosion inhibitors of mild steel in HCl medium", Chemical Engineering Communications **196** (2009) 1536.

[7] L. H. Madkour & S. K. Elroby, "Aminic nitrogen-bearing polydentate Schiff base compounds as corrosion inhibitors for iron in acidic and alkaline media: A combined experimental and DFT studies", Journal of corrosion science and engineering **17** (2014) 745.

[8] C. W. Chidieberea, C. E. Durua, JP. C. Mbagwub, "Application of computational chemistry in chemical reactivity: a review", Journal of the Nigerian Society of Physical Sciences **3** (2021) 292.

[9] B. T Ogunyemi, D. F. Latona & I. A. Adejoro, "Molecular modeling and quantitative structure–property relationships (QSPRs) of purine derivatives as corrosion inhibitor in acid medium", Scientific African **8** (2020) e00336. https://doi.org/10.1016/j.sciaf.2020.e00336

[10] R. Solmaz, "Investigation of the inhibition effect of 5-((E)-4-phenylbuta-1,3- dienylideneamino)-1,3,4-thiadiazole-2-thiol Schiff base on mild steel corrosion in hydrochloric acid", Corrosion. Science **52** (2010) 3321.

[11] S. Chitra, K. Parameswari & A. Selvaraj, "Dianiline Schiff Bases as Inhibitors of Mild Steel Corrosion in Acid Media", Int. J. Electrochem. Sci. **5** (2010) 1675.

[12] R. Solmaz, E. Altunbaşb & G. Kardas, "Adsorption and corrosion inhibition effect of 2-((5-mercapto-1,3,4-thiadiazol-2-ylimino) methyl)phenol Schiff base on mild steel, Gülfeza Kardaşb", *Materials Chemistry* and *Physics* **125** (2011) 796.

[13] M. Larouj, H. Lgaz, R. Salghi, S. Jodeh, M. Messali, M. Zougagh, H. Oudda & A. Chetouani, "Effect of chlorine group position on adsorption behavior and corrosion inhibition of Chlorobenzylideneamino-5-methyl-2, 4-dihydro-1, 2, 4-triazole3-thione Schiff bases: Experimental study", Moroccan *Journal of Chemistry* **4** (2016) 567.

[14] R. A. Prabhu, T. V. Venkatesha, A.V. Shanbhag, B. M. Praveen, G. M. Kulkarni & R.G. Kalkhambkar, "Quinol-2-thione compounds as corrosion inhibitors for mild steel in acid solution", *Materials Chemistry* and *Physics* **108** (2008) 283.

[15] A. S. Fonda, M. N. Mousa, F. I. Taha & A. I. Elneanaa, "The role of the thiosemicarbazide derivatives in the corrosion inhibition of Aluminium in hydrochloric acid", Corrosion Science **26** (1986) 719.

[16] W. J. Hehre & W. A Ohlinger, *Spartan '14*, Wavefunction, Inc., Irvine (2014).

[17] A. D. Becke, "Density-functional exchange-energy approximation with correct asymptotic behavior", Phys. Rev. A **38** (1988) 3098.

[18] A. D. Becke, "Density-functional thermochemistry, III. The role of exact exchange", *Journal of Chemical Physics* **98** (1993) 5648.

[19] R. G. Pearson, "Absolute electronegativity and hardness: application to inorganic chemistry", *Inorganic Chemistry* **27** (1988) 734.

[20] R. G. Pearson, "Absolute electronegativity and hardness correlated with the molecular orbital theory", Proceedings of the National Academy of Sciences **83** (1986) 8440.

[21] N. S. Abdelshafi, M. A. Sadik, M. A. Shoeib & S. A. Halim, "Corrosion inhibition of aluminum in 1 M HCl by novel pyrimidine derivatives, EFM measurements, DFT calculations and MD simulation Arabian Journal of Chemistry **15** (2022) 103459. https://doi.org/10.1016/j.arabjc.2021.103459

[22] R. G Parr, L.V. Szentpaly & S. Liu "Electrophilicity index", *Journal* of the American *Chemical Society.* **121** (1999) 1922.

[23] K. Anton, "Molecular modeling of organic corrosion inhibitors: Calculations, pitfalls, and conceptualization of molecule–surface bonding", Corrosion Science **193** (2021) 109650.

[24] Z. Zhou & H. V. Navangul, "Absolute hardness and aromaticity: MNDO study of benzenoid hydrocarbons", J. Phys. Org. Chem. **3** (1990) 784.

[25] I. Lukovits, E. Kálmán, & F. Zucchi, "Corrosion Inhibitors—Correlation Between Electronic Structure and Efficiency", Corrosion **57** (2001) 118.

[26] P. A. John, E. F. Awe, O. Adedirin & B. Olusupo, "Exploring structure indenture for some Schiff bases as anti-*Salmonella typhi* drugs: A QSAR Approach", International Journal of Advances in Scientific Research **2** (2016) 48.

[27] K. Roy, "A Primer on QSAR/QSPR Modeling", Springer Briefs in Molecular Science. (2015). https://doi.org/10.1007/978-3-319-17281-1_2.

[28] O. M. Akinlosotu1, B. T. Ogunyemi & B. B. Adeleke, "Substituent Effect on Bithiophene-Bipyridine Organic Conjugated Systems: Theoretical Investigation", Advanced Journal of Chemistry-Section A, **5** (2022) 70.

[29] L. H. Madkour & I. H. Elshamy, "Experimental and Computational Studies on the Inhibition Performances of Benzimidazole and Its Derivatives

for the Corrosion of Copper in Nitric Acid", International Journal of Industrial Chemistry **7** (2016) 195

[30] M. M. Kabanda, S. K. Shukla, A.K Singh, L. C. Murulana, & E.E. Ebenso, "Electrochemical and Quantum Chemical Studies on Calmagite and Fast Sulphone Black F Dyes as Corrosion Inhibition for Mild Steel in Hydrochloric Medium", International Journal of Electrochemical Science **7** (2012) 8813.

[31] K. Kathirvel, B. Thirumalairaj, & M. Jaganathan, "Quantum Chemical Studies on the Corrosion Inhibition of Mild Steel by Piperidin-4-One Derivatives in 1 M H_3PO_4 Open Journal of Metal **4** (2014) 73.

[32] D. Datta, "Geometric mean principle for hardness equalization: a corollary of Sanderson's geometric mean principle of electronegativity equalization", Journal of Physical Chemistry **90** (1986) 4216.

[33] R. G. Pearson, "The principle of maximum hardness", Account of Chemical Research **26** (1993) 250.

[34] S. Kaya & C. Kaya, "A new method for calculation of molecular hardness: A theoretical study", computational and theoretical chemistry **1060** (2015) 66. https://doi.org/10.1016/j.comptc.2015.03.004

[35] C. Kaya, *Inorganic chemistry 1 and 2*, Palme Publishing, Ankara, (2011).

[36] M. Gholami, I. Danaee, M. M Hosein & R. A. Mehdi, "Correlated ab Initio and Electroanalytical Study on Inhibition Behavior of 2-Mercaptobenzothiazole and Its Thiole−Thione Tautomerism Effect for the Corrosion of Steel (API 5L X52) in Sulphuric Acid Solution", *Industrial & Engineering Chemistry Research* **52** (2011) 14875.

[37] B. T. Ogunyemi, D. F. Latona, A. A. Ayinde & I. A. Adejoro, "Theoretical Investigation to Corrosion Inhibition Efficiency of Some Chloroquine Derivatives Using Density Functional Theory", Advance Journal of Chemistry-section A **3** (2020) 485. https://doi.org/10.33945/SAMI/AJCA.2020.4.10

[38] E. E. Ebenso, D.A. Isabirye, & N. O. Eddy, "Adsorption and quantum chemical studies on the inhibition potentials of some thiosemicarbazides for the corrosion of mild steel in acidic medium", International Journal of Molecular Science **11** (2010) 2473. https://doi.org/10.3390/ijms11062473

[39] X. Li, S. Deng, H. Fu & T. Li, "Adsorption and Inhibition Effect of 6-Benzylaminopurine on Cold Rolled Steel in 1.0 M HCl", Electrochimica Acta **54** (2009) 4089.

[40] N. O. Eddy & E. E. Ebenso, "quantum chemical studies on the inhibition potentials of some penicillin compounds for the corrosion of mild steel in 0.1 m HCl" Journal of Molecular Modelling **16** (2010) 1291.

[41] B. T. Ogunyemi & G. S. Borisade, "Theoretical Modeling of Iminoisatin Derivatives as Corrosion Inhibitors of Steel in Acid Solution", FUDMA Journal of Sciences (FJS) **4** (2020) 672. https://doi.org/10.33003/fjs-2020-0403-372

[42] K. Adardour, R. Touir, M. Elbakri et al., "*Thermodynamic study* of *mild steel corrosion* in *hydrochloric acid* by *new class synthesized quinoxaline derivatives*: *Part II"*, *Research on Chemical* I*ntermediate **39** (2013) 4175.* https://doi.org/10.1007/s11164-012-0934-x

[43] M. Sahin, G. Gece, E. Karci & S. Bilgic, "Experimental and theoretical study of the effect of some heterocyclic compounds on the corrosion of low carbon steel in 3.5% NaCl medium", *Journal of Applied Electrochemistry* **38** (2008) 809.

[44] M. E. Elshakre, H. H. Alalawy, M. I. Awad & B. E. El-Anadouli, "On the role of the electronic states of corrosion inhibitors: Quantum chemical-electrochemical correlation study on urea derivatives", Corrosion Science **124** (2017) 121.

[45] I. B. Obot, N. O. Obi-Egbedi, & S. A. Umeren, "Adsorption characteristics and corrosion inhibitive properties of clotrimazole for aluminium corrosion in hydrochloric acid", *International Journal* of Electrochemical *Science* **4** (2009) 863.